

# The Role of Avoidance and Learning Behaviours on the Formation and Movement of Biological Aggregations

R. Eftimie<sup>1</sup> \*, A. Coulier<sup>2</sup>

<sup>1</sup> Division of Mathematics, University of Dundee, Dundee, DD1 4NR, UK

<sup>2</sup> Institut National des Sciences Appliquées de Rouen, 76800, Saint-Étienne-du-Rouvray, France

**Abstract.** Communication forms the basis of any animal aggregation. However, not all organisms communicate the same way. Moreover, different psychological and physiological characteristics of individuals can lead to avoidance behaviours between different individuals. This can have implications on the formation and structure of large biological aggregations. In this article, we use a mathematical model to investigate the effects of avoidance behaviour by a subpopulation, on the spatial dynamics of the whole population. We show that avoidance (exhibited even by a small fraction of the population) can alter the spatio-temporal patterns of the whole groups, leading to new patterns difficult to predict from the case without avoidance. Generally, these patterns show the segregation of the populations into different aggregations (spatially separated) or inside the same aggregation. Moreover, we investigate numerically the situation where individuals can learn to tolerate their neighbours. In this case, we observe an unexpected spatial segregation inside moving aggregations of individuals that tolerate their neighbours and those that avoid their neighbours.

**Keywords and phrases:** communication, discrimination and avoidance, tolerance, nonlocal mathematical model

**Mathematics Subject Classification:** 35Q53, 34B20, 35G31

## 1. Introduction

Research on animal communities has started to highlight the importance of information transfer (i.e., communication) between individuals in mixed-species aggregations, and how this transfer influences the structure of the ecological aggregations [15, 21, 22]. Although there is evidence of language-based segregation in human societies [23], or information-based formation of mixed-species aggregations [21], segregation of animal groups has been discussed mainly in the context of different body sizes [30, 34], parasite infections [2], level of hunger [25] or swimming speed [28]. A recent theoretical study showed the segregation of individuals inside biological aggregations based on different communication/perception mechanisms used by these individuals [15].

---

\*Corresponding author. E-mail: [reftimie@maths.dundee.ac.uk](mailto:reftimie@maths.dundee.ac.uk)

A type of behaviour (also related to how individuals perceive each other) that leads to the spatial segregation of group members, is the inter-individual avoidance behaviour. Avoidance is quite common in socially structured communities, as seen for example, in chimpanzees [33]. Also birds can display avoidance behaviours [38, 39]. While avoidance against particular individuals of the groups (as seen in birds with different plumage [39]) has been observed and investigated at the individual level, its role on the group-level dynamics and on the types of spatial aggregation structures that it creates is still not very clear.

Social biological communities formed of individuals belonging to different species can exhibit also learning behaviours [22, 26, 31]. For example, individuals from two species of chickadees (belonging to a mixed flock) have been shown to learn from each other the location of feeding places [26]. It is therefore reasonable to assume (at least for social animals) that individuals that avoid some of their neighbours could learn to tolerate them, upon interactions with more tolerant members of the community.

The goal of this paper is to investigate numerically the effect of avoidance behaviours and learning tolerance behaviours on the types of aggregations exhibited by biological groups – an investigation not attempted before by the existent mathematical models (see, for example, the various models in [1, 3–5, 9–12, 20, 29, 32, 35–37, 41] and the references therein). Moreover, we aim to investigate the effect of these behaviours on the spatial distributions of (tolerant and non-tolerant) individuals inside these aggregations. To this end, we will start with a mathematical model introduced in [15], which describes nonlocal social interactions among individuals belonging to two subpopulations,  $u$  and  $v$ , each using a different communication mechanism to interact with neighbours. In [15] it was assumed that individuals interact in a similar manner with neighbours from their own subpopulation as well as with neighbours from the other subpopulation. Here, we will assume that there is an avoidance behaviour between individuals belonging to the two subpopulations. In particular, we will assume that one population (which can perceive all of its neighbours via a combination of multiple sensory mechanisms; e.g., visual and auditory stimuli) will avoid the second population (which, possibly due to some physiological impairment, uses only some sensory mechanisms, e.g., directional auditory stimuli, to perceive *only* those neighbours moving towards it). This mathematical model will then be used to investigate the shape and structure of aggregation patterns displayed during avoidance behaviours. In this study, we will also investigate numerically the situation where individuals can learn to change their avoidance behaviour upon interactions with their more tolerant neighbours. Again, our focus will be on the shape and structure of the patterns displayed during avoidance and learning behaviours.

This paper is structured as follows. We start in Section 2 with the description of the avoidance model. In Section 3, we then investigate the long-term dynamics of this model. In Section 4 we generalise the avoidance model to include also learning behaviours, and investigate numerically some of the spatio-temporal patterns exhibited by this model. We conclude with a discussion in Section 5.

## 2. Description of “avoidance” model

The following model was introduced in [15] to describe the dynamics (on a 1D domain) of two populations  $u^\pm$  and  $v^\pm$  that interact using different communication mechanisms:

$$\frac{\partial u^+}{\partial t} + \gamma \frac{\partial u^+}{\partial x} = -\lambda_u^+[u^+, u^-, v^+, v^-]u^+ + \lambda_u^-[u^+, u^-, v^+, v^-]u^-, \quad (2.1a)$$

$$\frac{\partial u^-}{\partial t} - \gamma \frac{\partial u^-}{\partial x} = \lambda_u^+[u^+, u^-, v^+, v^-]u^+ - \lambda_u^-[u^+, u^-, v^+, v^-]u^-, \quad (2.1b)$$

$$\frac{\partial v^+}{\partial t} + \gamma \frac{\partial v^+}{\partial x} = -\lambda_v^+[u^+, u^-, v^+, v^-]v^+ + \lambda_v^-[u^+, u^-, v^+, v^-]v^-, \quad (2.1c)$$

$$\frac{\partial v^-}{\partial t} - \gamma \frac{\partial v^-}{\partial x} = \lambda_v^+[u^+, u^-, v^+, v^-]v^+ - \lambda_v^-[u^+, u^-, v^+, v^-]v^-. \quad (2.1d)$$

Here,  $u^+$  and  $v^+$  are the densities of the right-moving individuals in the two subpopulations, while  $u^-$  and  $v^-$  are the densities of the left-moving individuals in these subpopulations. We assume that the individuals in both subpopulations move at the same constant speed  $\gamma$ , and change their direction of movement upon interactions with neighbours. The turning rates  $\lambda_{u,v}^\pm$  are described by

$$\lambda_{u,v}^\pm = \lambda_1 + \lambda_2 f(y_r^{u,v;\pm} - y_a^{u,v;\pm} + y_{al}^{u,v;\pm}), \quad (2.2)$$

with  $\lambda_1$  and  $\lambda_2$  approximating the random turning and directed turning rates, respectively [18]. Function  $f$  models the probability of directed turning in response to nonlocal social interactions: attraction towards neighbours further away, repulsion from neighbours at very close distances, and alignment with neighbours at intermediate distances. For biological realism,  $f$  is a positive and increasing function of signals perceived from neighbours. An example of such function (which will be used throughout this article) is  $f(u) = 0.5 + 0.5 \tanh(u - 2)$ . Here, the argument  $u - 2$  ensures that when  $u \approx 0$  (i.e., no neighbours around) we have  $0.5 + 0.5 \tanh(u - 2) \approx 0$ , and the turning is mainly random. Finally, the terms  $y_j^{u,v;\pm}$ ,  $j = r, a, al$ , in (2.2) describe the nonlocal social interactions with neighbours, where the upper indices  $u, v$  indicate whether the turning rates correspond to the  $u$  or  $v$  subpopulations, while the lower indices  $j$  indicate whether the turning is the result of repulsive ( $r$ ), attractive ( $a$ ) or alignment ( $al$ ) interactions. These social interactions depend on inter-individual communication, namely whether individuals can emit/perceive information to/from their neighbours. Figure 1 shows examples of two communication mechanisms, M2 and M4 that were previously introduced in [16]. For these mechanisms, we assume that population  $u$  communicates via M2 – see Figure 1(a) – and thus can perceive (e.g., via a combination of visual and auditory signals) *all* their neighbours ahead and behind them within a certain perception range. On the other hand, population  $v$  communicates via mechanisms M4 – see Figure 1(b) – and can perceive (e.g., via directional sound signals) *only* those neighbours moving towards them (see, for example, studies on directional sound communication in birds [40] and killer whales [27]). Once they perceive these neighbours, the individuals can decide to avoid them or not. For the purpose of this article, we assume that population  $u$  avoids population  $v$ , while population  $v$  does not avoid population  $u$ . In particular,  $u^\pm$  are attracted only to other  $u^\pm$  positioned inside the attraction range, while  $v^\pm$  are attracted to both  $v^\pm$  and  $u^\pm$  (i.e.,  $v^\pm$  are the *tolerant* population). Similarly, population  $u^\pm$  aligns only with other  $u^\pm$ , while population  $v^\pm$  aligns with both  $u^\pm$  and  $v^\pm$ . For the repulsive interactions:  $u^\pm$  and  $v^\pm$  are repelled by both subpopulations inside the repulsion range. These assumptions can be translated into mathematical equations for the social interactions – see Table 1.

To complete the description of model (2.1), we assume that the domain is finite, of length  $L$ :  $[0, L]$ . The boundary conditions are periodic (as used in some experimental settings investigating the movement of self-organised biological aggregations [6]):

$$u^+(0, t) = u^+(L, t), \quad u^-(L, t) = u^-(0, t), \quad (2.3a)$$

$$v^+(0, t) = v^+(L, t), \quad v^-(L, t) = v^-(0, t). \quad (2.3b)$$

These boundary conditions are used throughout the rest of the paper.

We emphasise that in this article we will focus only on these two communication mechanisms, M2 and M4, described in Figure 1. However, other types of mechanisms have been described in [15, 16]. Moreover, the combination of various communication mechanisms by different subpopulations has been investigated previously in [15], in the context of tolerant behaviours: all individuals interacted in a similar manner with neighbours from their own subpopulation as well as with neighbours from the other subpopulation. However, it is not the purpose of this article to investigate avoidance behaviours in all communication models studied in [15]. Rather it is to focus on a particular sub-model (we chose here M2&M4 since in [15] it showed a wide range of various patterns) and to investigate how behaviours such as avoidance or learning to tolerate neighbours affect the spatial distribution of individuals in a group.

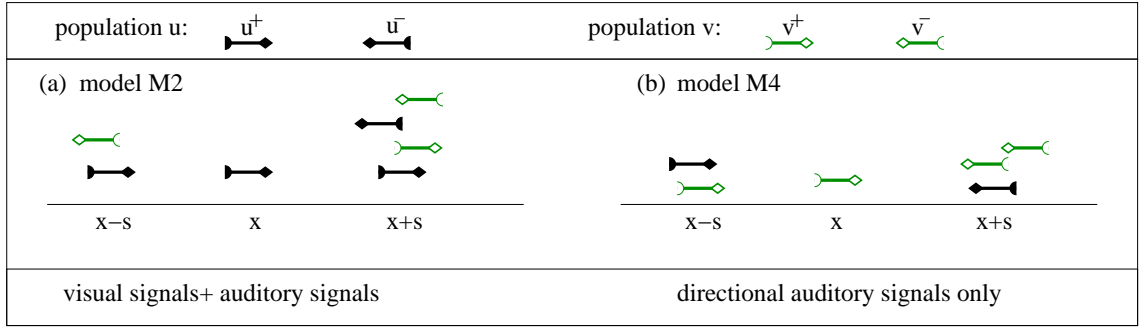


FIGURE 1. Caricature description of two communication mechanisms: (a) model M2 from [16], where the right-moving reference individual at  $x$  can perceive *all* of its neighbours positioned ahead at  $x + s$  and behind at  $x - s$ ; (b) model M4 from [16], where the right-moving reference individual at  $x$  can perceive *only* those neighbours moving towards it (neighbours who might communicate via directional auditory signals, as in bird communities or killer whale communities [27,40]). Similar descriptions hold also for left-moving reference individuals.

TABLE 1. Nonlocal social interaction terms for populations  $u$  (which communicates via M2) and population  $v$  (which communicates via M4). We assume that  $u^\pm$  are neither attracted to  $v^\pm$  (inside the attraction range), nor do they align with the movement direction of  $v^\pm$  neighbours (inside the alignment range). However,  $u^\pm$  will be repelled by both  $v^\pm$  and  $u^\pm$  within the repulsion range. In contrast,  $v^\pm$  interact similarly with all their  $u^\pm$  and  $v^\pm$  neighbours.  $K_r$ ,  $K_a$  and  $K_{al}$  are kernels describing the spatial ranges for the repulsive, attractive and alignment interactions, respectively. Throughout this study we use  $K_j(s) = (1/2\pi m_j^2) \exp(-(s - s_j)^2/(2m_j^2))$ , with  $j = r, al, a$ , and  $m_j = s_j/8$ . Finally,  $q_j$ ,  $j = r, al, a$ , are the magnitudes of the social interactions.

| Population | Interaction terms: repulsion ( $y_r^\pm$ ), attraction ( $y_a^\pm$ ), alignment ( $y_{al}^\pm$ )   |
|------------|--|
| $u$        | $y_r^{u;\pm} = y_r^{M2;\pm} = \pm q_r \int_0^L K_r(s) (u^+(x+s) + u^-(x+s) - u^+(x-s) - u^-(x-s) + v^+(x+s) + v^-(x+s) - v^+(x-s) - v^-(x-s)) ds;$ $y_a^{u;\pm} = y_a^{M2;\pm} = \pm q_a \int_0^L K_a(s) (u^+(x+s) + u^-(x+s) - u^+(x-s) - u^-(x-s)) ds;$ $y_{al}^{u;\pm} = y_{al}^{M2;\pm} = \pm q_{al} \int_0^L K_{al}(s) (u^-(x+s) + u^-(x-s) - u^+(x+s) - u^+(x-s)) ds;$ |
| $v$        | $y_r^{v;\pm} = y_r^{M4;\pm} = \pm q_r \int_0^L K_r(s) (v^-(x+s) + u^-(x+s) - v^+(x-s) - u^+(x-s)) ds;$ $y_a^{v;\pm} = y_a^{M4;\pm} = \pm q_a \int_0^L K_a(s) (v^-(x+s) + u^-(x+s) - v^+(x-s) - u^+(x-s)) ds;$ $y_{al}^{v;\pm} = y_{al}^{M4;\pm} = \pm q_{al} \int_0^L K_{al}(s) (v^-(x+s) + u^-(x+s) - v^+(x-s) - u^+(x-s)) ds.$   |

### 3. Results for the “avoidance” model

In the following, we investigate the long-term behaviour of model (2.1) that incorporates avoidance behaviours. We first study the number and type of spatially homogeneous steady states, as we vary the sizes of the two populations,  $u$  and  $v$ . Then, we investigate numerically the spatial and spatio-temporal patterns exhibited by these populations.

#### 3.1. Spatially homogeneous steady states for the “avoidance” model

First, we focus on the long-term behaviour of these models, and investigate the spatially homogeneous steady states (i.e., states characterised by individuals spread evenly over the whole domain). We call *non-polarised states* those steady states formed of an equal number of left-facing and right-facing individuals. If we denote by  $A = (1/L) \int_0^L (u^+(s) + u^-(s)) ds$  the total density for population  $u$  (with  $L$  being domain

length), and by  $B = (1/L) \int_0^L (v^+(s) + v^-(s)) ds$  the total density for population  $v$ , then a non-polarised state for model (2.1) would be described by  $(u^+, u^-, v^+, v^-) = (A/2, A/2, B/2, B/2)$ . We call *polarised states* those states formed of a larger number of individuals facing in one direction compared to the opposite direction; for example  $(u^+, u^-) = (u^*, u^{**})$  with  $u^* > A/2$  and  $u^{**} < A/2$ , or  $(v^+, v^-) = (v^*, v^{**})$  with  $v^* < B/2$  and  $v^{**} > B/2$ . Note that there could be different degrees of polarisation: from mildly-polarised states (where  $u^* \approx u^{**}$  &  $v^* \approx v^{**}$ ), to medium-polarised states (where, for example,  $u^* \approx u^{**}$  &  $v^* < v^{**}$ ), and eventually to strongly-polarised states (where, for example,  $u^*, v^* \gg A/2$  &  $u^{**}, v^{**} \ll A/2$ ). We will re-discuss some of these polarised states at the end of this subsection. To reduce the number of variables, in the following we will consider  $u^{**} = A - u^*$  and  $v^{**} = B - v^*$ .

Figure 2 shows the number of homogeneous steady states displayed by model (2.1) for the case  $A = B$  (i.e., same total density for populations  $u$  and  $v$ ), and for some particular parameter values for the magnitudes of the social interactions. Here, the black, continuous lines are the solutions of

$$-\lambda_u^+[u^*, A - u^*, v^*, B - v^*]u^* + \lambda_u^-[u^*, A - u^*, v^*, B - v^*](A - u^*) = 0. \quad (3.1)$$

For the model with avoidance behaviour, since the repulsion interactions calculated at the steady states are zero, the turning rates  $\lambda_u^\pm$  do not depend anymore on  $v^*$  and thus equation (3.1) can be solved for  $u^*$  (hence the vertical lines in Figure 2 that are constant for all  $v^*$  values). The red, dashed curves in Figure 2 are the solutions of

$$-\lambda_v^+[u^*, A - u^*, v^*, B - v^*]v^* + \lambda_v^-[u^*, A - u^*, v^*, B - v^*](B - v^*) = 0. \quad (3.2)$$

We observe in Figure 2 that the introduction of an avoidance behaviour (Figure 2 (a)-(e)) leads to a larger number of spatially homogeneous steady states (7 states), compared to the case without avoidance behaviour that was studied in [15] (Figure 2(a')-(e'); 5 states). For other parameter values, avoidance behaviours can lead to many more steady states (e.g., for  $A = 0.4$ ,  $B = 0.8$ ,  $q_r = q_a = 2$ ,  $q_{al} = 6.7$  one can obtain 13 different steady states; not shown here). This large number of steady states has implications on understanding the dynamics of the model. Since multiple states can become stable at the same time (i.e., multi-stability phenomena), it becomes difficult to predict which of these homogeneous states are approached by the solutions of the model. We note, however, that as we increase the magnitude of attractive interactions (e.g.,  $q_a = 6.7$  but  $q_r = q_a = 2$ ) the models with and without avoidance show the same number of possible spatially homogeneous steady states (namely 1, 3 or 5 states).

To summarise the results on the homogeneous steady states: (i) for any  $A > 0$ , there is always one non-polarised state (e.g., in Figure 2 (a)-(a') this state is  $(u^+, u^-, v^+, v^-) = (0.3, 0.3, 0.3, 0.3)$ , with  $A/2 = 0.3$ ); (ii) for medium to large  $A$ , there is usually a multitude of steady states (e.g., for  $A = B = 1.95$ , model (2.1) can exhibit up to 7 coexistent steady states, 6 of which are polarised states); (c) for very large populations ( $A = B \rightarrow \infty$ ), model (2.1) exhibits 5 steady states:

- one non-polarised state  $(u^*, A - u^*, v^*, A - v^*) = (A/2, A/2, A/2, A/2)$ ;
- two strongly-polarised states  $(u^*, A - u^*, v^*, A - v^*)$  with  $u^* = v^* = A\lambda_1/(2\lambda_1 + \lambda_2)$  (in Figure 2(e'):  $u^* = v^* = 0.76823$ ). We call these states “strongly-polarised” since  $u^*, v^* \ll A/2$ .
- two medium-polarised states  $(u^*, A - u^*, v^*, A - v^*)$  with  $u^* = A/2$  and  $v^* = A\lambda_1/(2\lambda_1 + \lambda_2)$  (in Figure 2(e'):  $u^* = 2.5$ ,  $v^* = 0.76823$ ). We call these states “medium polarised” since  $v^* \ll A/2$  but  $u^* = A/2$ .

As we will discuss in the next Section, for the parameter values investigated in this article, the dynamics of system (2.1) will approach only the non-polarised state.

### 3.2. Pattern formation with the “avoidance” model

Next, we focus on a particular parameter space and investigate numerically the dynamics of model (2.1). We emphasise here that it is not the goal of this article to investigate the whole parameter space for changes in model dynamics. Rather it is to provide the reader with a hypothesis on the role of inter-individual avoidance on the formation and structure of different aggregation patterns.

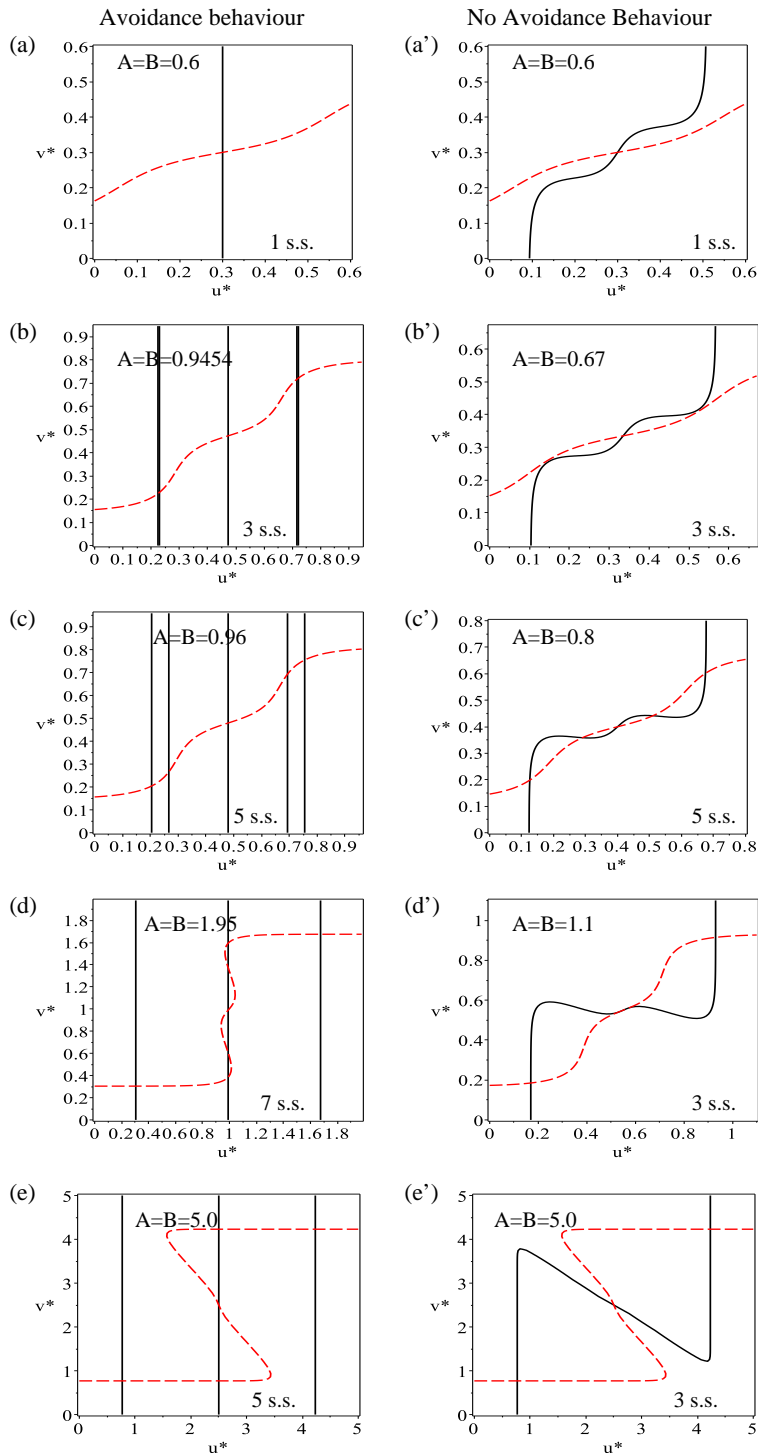


FIGURE 2. Number of spatially homogeneous steady states (s.s.) exhibited by system (2.1) with avoidance (panels (a)–(e)). For comparison purposes, in panels (a')–(e') we also show the steady states for the model without avoidance introduced in [15]. We assume here that  $u$  and  $v$  populations have the same total density:  $A = B$ . The rest of parameters are  $\lambda_1 = 0.2$ ,  $\lambda_2 = 0.9$ ,  $q_a = q_r = q_{al} = 2.0$ .

For the numerical simulations, we use a simple upwind/downwind scheme to discretise the model equations. The nonlocal integrals are discretised using Simpson's method. The initial conditions are random perturbations (of maximum amplitude 0.02) of the spatially homogeneous steady states  $u^\pm = u^* + \text{rand}(0..0.02)$ ,  $v^\pm = v^* + \text{rand}(0..0.02)$ . The perturbations are applied at every discrete spatial location. Finally, the boundary conditions are periodic (see 2.3). Simulations are run up to  $t \approx 1500 - 2000$ , by which time the transient behaviour vanishes and the system approaches a persistent state. We fix here all model parameters ( $q_a = 6.7$ ,  $q_r = 2$ ,  $q_{al} = 2$ ,  $\gamma = 0.1$ ,  $L = 10$ ,  $s_a = 1$ ,  $s_{al} = 0.5$ ,  $s_r = 0.25$ ) and vary only the initial population sizes. This allows us to discuss the importance of population size on the types of patterns exhibited by model (2.1).

Overall, model (2.1) can exhibit (i) patterns where the two populations segregate into two groups spatially separated, and (ii) patterns where the two populations remain in the same group, but they are spatially segregated:

(i) *Patterns with group separation.* Figure 3 shows some of the patterns displayed by the ‘‘avoidance’’ model (2.1), where populations  $u$  and  $v$  separate into spatially distinct groups. Among these patterns we observe: (a)–(d) zigzags + stationary pulses, and (e)–(h) travelling zigzags. Note that for moving aggregations (as in panels (e)–(h)), population  $u = u^+ + u^-$  is always at the front, while population  $v = v^+ + v^-$  is trailing behind. It seems that these patterns occur when population  $u$  is much lower than population  $v$ . In this case,  $u^\pm$  move away from  $v^\pm$ , and because they are at so low values, population  $v^\pm$  is not attracted very strongly to them.

(ii) *Patterns without group separation.* Figure 4 shows some of the patterns displayed by the avoidance model (2.1), where populations  $u$  and  $v$  belong to the same group. Among these patterns we observe, for example, different types of semi-zigzag pulses (Figure 4(a),(b)) or wavy pulses (Figure 4(c)). The two types of semi-zigzags shown in panels (a) and (b) are: (a) type 2, where rectilinear movement in one direction alternates with a short movement in the opposite direction, and (b) type 1, where rectilinear movement in one direction alternates with short periods of stationary pulses.

Again, we observe that for moving groups, population  $u$  is slightly ahead of population  $v$ . In [15] was shown that in the absence of avoidance behaviours, the structure of the moving groups is reversed, with population  $v$  at the front of the group and population  $u$  at the back of the group. We will return to this aspect in Figure 9 (Section 4). For stationary groups, population  $u$  is positioned in the middle of the aggregation, while population  $v$  is positioned at the edge of the aggregation (see Figure 4(c)). This results holds both in the presence and the absence of avoidance behaviours [15].

We summarise in Figure 5(a) all patterns exhibited by model (2.1) in a particular parameter space given by the initial population sizes:  $(u^*, v^*) \in (0, 1)$ . For comparison purposes, in Figure 5(b) we show the patterns obtained (in the same parameter space) in the absence of avoidance behaviours (see also [15]). (For a description of all types of patterns exhibited by this class of nonlocal hyperbolic models see also [13, 15].) First, we note in Figure 5(a) the difference between the patterns obtained with avoidance behaviour and the patterns without avoidance behaviour. In addition to the different ranges in the population size where one can see stationary pulses, zigzags or travelling pulses, we also notice the difference in the types of patterns caused by avoidance behaviour. In particular, we can obtain travelling zigzags (see Figure 3(e)), a type of pattern not displayed by the model without avoidance. Moreover, we notice that some patterns can occur only for some population sizes. For example, avoidance leads to travelling pulses only for small  $u^*$  and  $v^*$ , and to travelling zigzags only for very small  $u^*$  and large  $v^*$ .

We observe in Figure 5(b) that the model without avoidance can exhibit chaotic zigzags for  $u^* = 0.1$ ,  $v^* = 1.0$  (these zigzags are described in [15]). Similar chaotic zigzags are possible also for the model with avoidance (not shown here). However, for model (2.1), the chaotic zigzags are unstable and they actually bifurcate to travelling zigzags, as described in Figure 3(e). Another observation refers to the single patterns obtained in regions dominated by other patterns. For example, stationary pulses can be obtained for the avoidance behaviour when  $(u^*, v^*) = (0.65, 0.65)$  (in Figure 3(a)), while the neighbourhood of this point is dominated by semi-zigzag travelling pulses. This suggests the co-existence of multiple solution

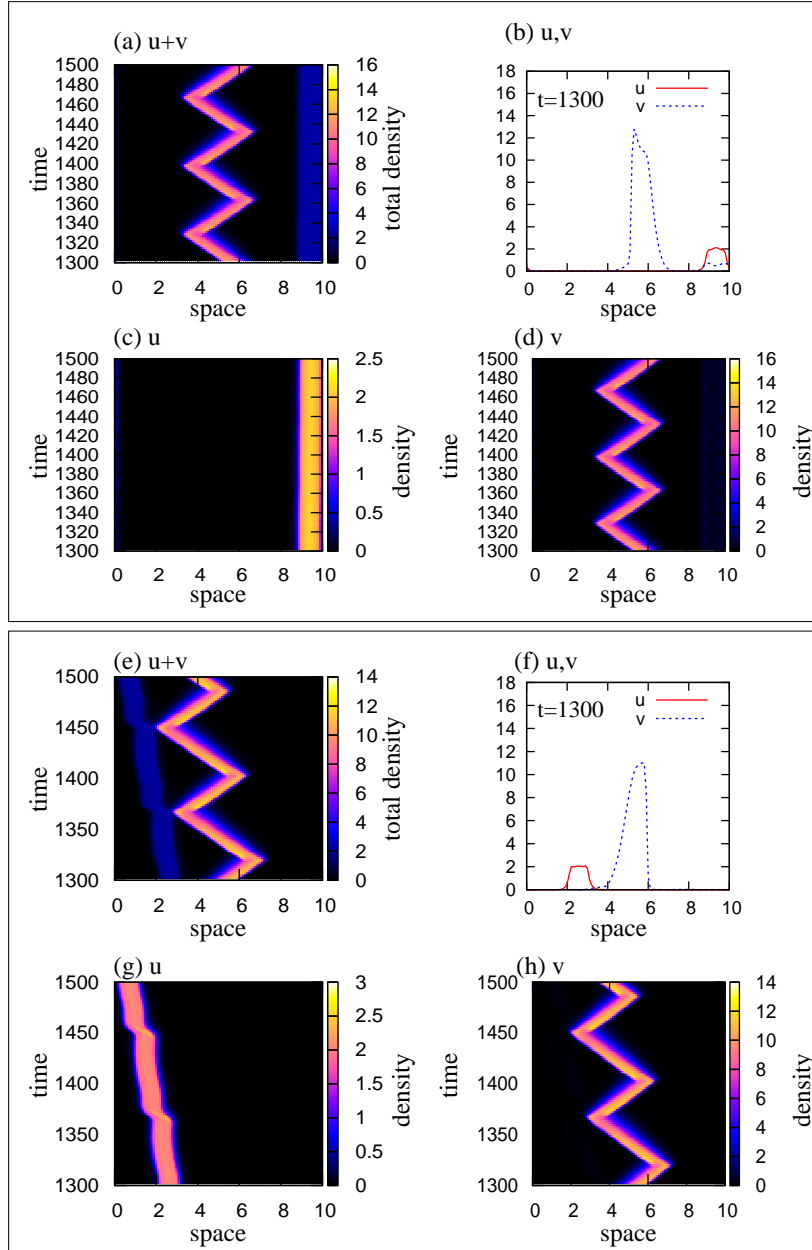


FIGURE 3. Examples of patterns (with group separation) obtained with “avoidance” model (2.1), for different parameter values. Panels (a), (e) show the total population density  $u + v$ ; panels (b), (f) show the space distribution of populations  $u$  and  $v$ , at a particular time step ( $t = 1300$ ); panels (c), (g) show the density for subpopulation  $u = u^+ + u^-$ ; panels (d), (h) show the density for subpopulation  $v = v^+ + v^-$ . Initial population sizes: (a)–(d) zigzags+stationary pulses:  $u^* = 0.1$ ,  $v^* = 0.7$ ; (e)–(h) travelling zigzags:  $u^* = 0.1$ ,  $v^* = 0.65$ . The rest of parameter values are:  $q_a = 6.7$ ,  $q_{al} = q_r = 2$ ,  $\gamma = 0.1$ ,  $\lambda_1 = 0.2$ ,  $\lambda_2 = 0.9$ ,  $s_r = 0.25$ ,  $s_{al} = 0.5$ ,  $s_a = 1$ ,  $L = 10$ .

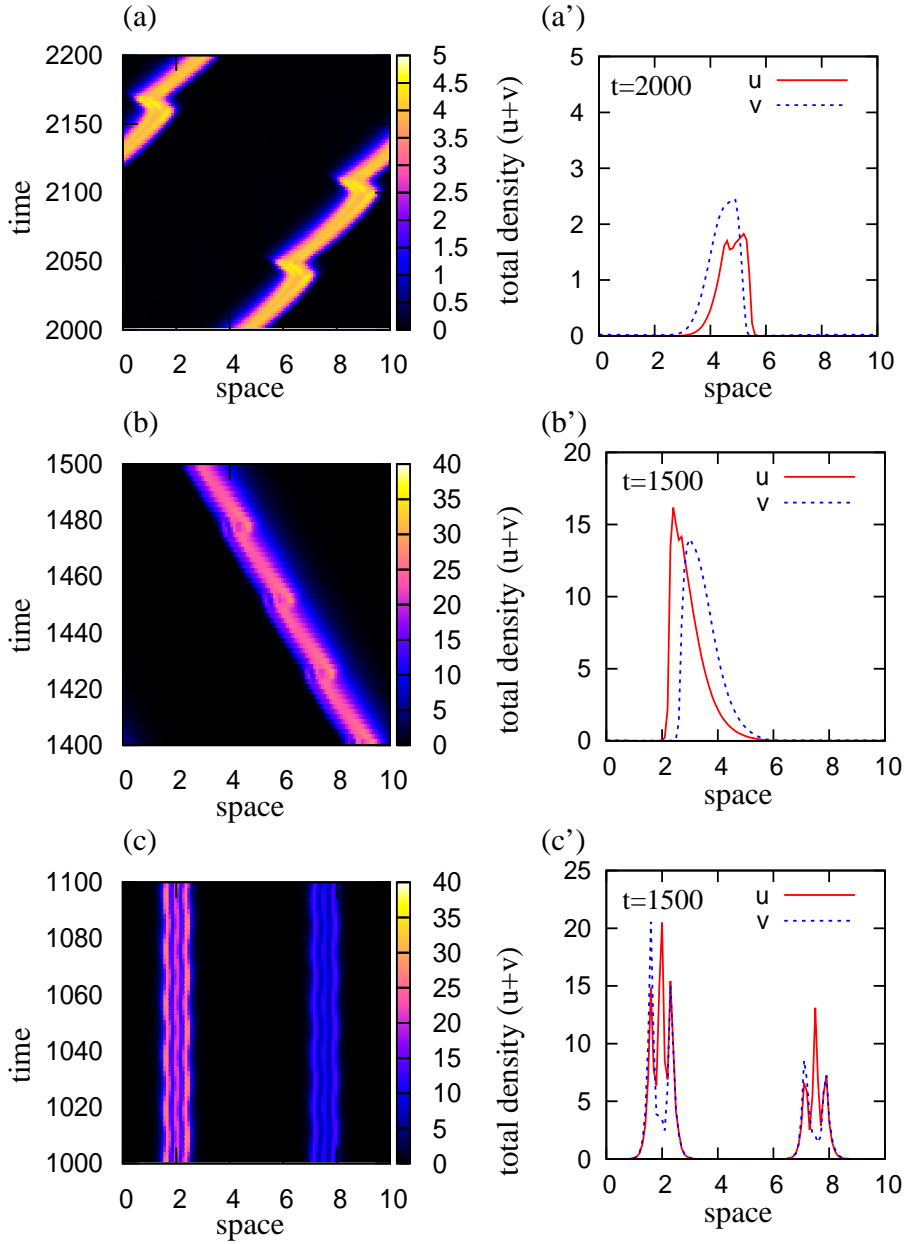


FIGURE 4. Examples of patterns (without group separation) obtained with the avoidance model (2.1), for different parameter values. Panels (a)–(c) show the total population density  $u + v$ , panels (a')–(c') show the spatial distribution of the densities for subpopulations  $u$  and  $v$ , at some particular time steps. Initial population sizes: (a),(a')  $u^* = 0.1$ ,  $v^* = 0.15$ ; (b),(b')  $u^* = 0.85$ ,  $v^* = 0.9$ ; (c),(c')  $u^* = 0.95$ ,  $v^* = 0.75$ . The rest of parameter values are:  $q_a = 6.7$ ,  $q_{al} = q_r = 2$ ,  $\gamma = 0.1$ ,  $\lambda_1 = 0.2$ ,  $\lambda_2 = 0.9$ ,  $s_r = 0.25$ ,  $s_{al} = 0.5$ ,  $s_a = 0.5$ ,  $L = 10$ .

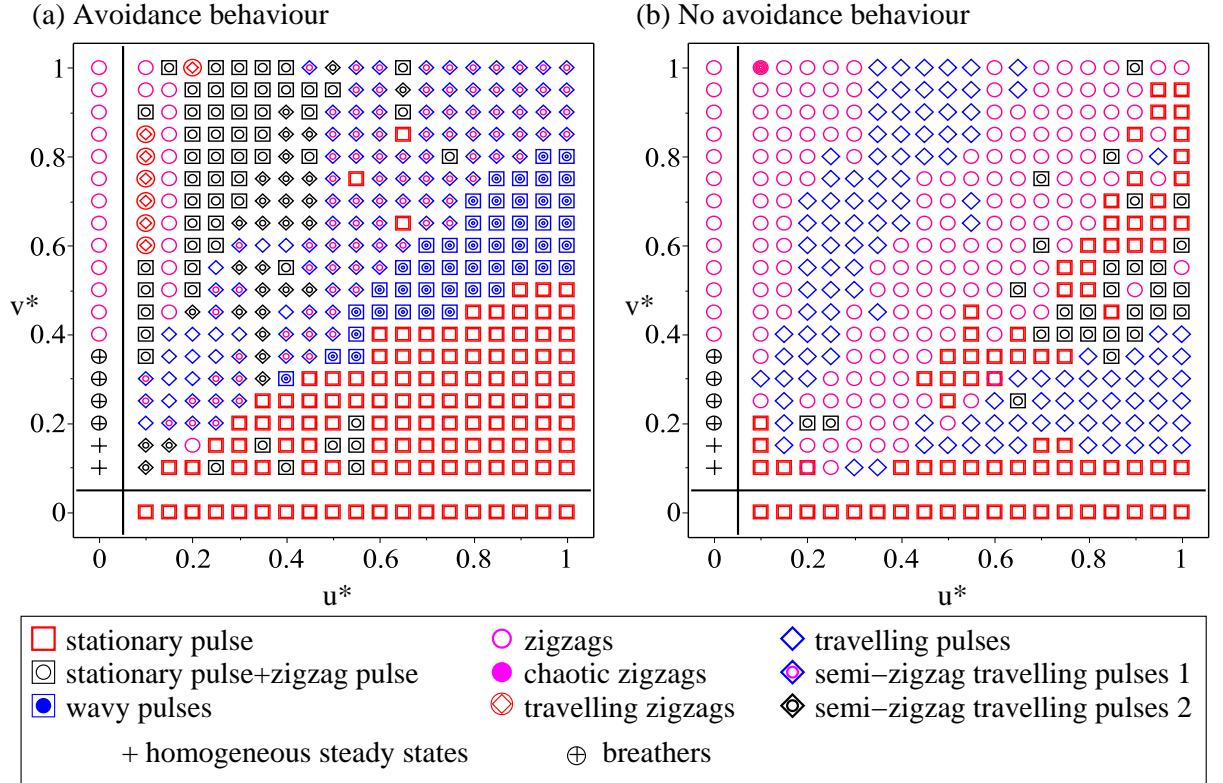


FIGURE 5. Comparison between patterns obtained (a) with avoidance behaviour (model (2.1)), and (b) without avoidance behaviour (as in [15]), for different initial population sizes  $u^+(0, x) = u^-(0, x) = u^*$  and  $v^+(0, x) = v^-(0, x) = v^*$ .

branches near these points, and whichever solution is chosen (either stationary pulses or semi-zigzag travelling pulses) depends on the initial data.

Finally, note in Figure 5 the presence of spatially homogeneous steady states (denoted by “+”) that occur for  $u^* = 0$  and  $v^* < 0.2$ . These are non-polarised states:  $(u^+, u^-, v^+, v^-) = (A/2, A/2, B/2, B/2)$ .

For  $q_a = q_r = q_{al} = 2.0$ , it was shown in [15] that the model without avoidance can approach the same non-polarised state  $(A/2, A/2, B/2, B/2)$ , for a much larger range of initial population sizes. In Figure 6(a) we summarise the dynamics of model (2.1) with avoidance behaviours, for one particular case:  $v^* = 0.8$  and  $u^* \in (0.1, 1.0)$ ). For comparison purposes, we also show the dynamics of the model without avoidance behaviours (introduced in [15]). Note the different ranges for  $u^*$  (for the models with and without avoidance) where one can obtain spatially homogeneous states and travelling pulses. We can conclude from here that at large population sizes ( $u^* \geq 0.4$ ), avoidance behaviours could lead to the formation of biological aggregations (here travelling pulses). At small population sizes ( $u^* < 0.4$ ), avoidance behaviours could lead to the dispersal of existent aggregations (and the formation of spatially homogeneous steady states).

#### 4. Learning aspects of social interactions

Let us focus now on population  $u$  that communicates via M2, and assume that while the majority of individuals display avoidance behaviours, there are a few who do not avoid their neighbours. Denote by  $u_1^\pm$  the density of individuals that avoid their neighbours, and by  $u_2^\pm$  the density of individuals that tolerate their neighbours. Therefore,  $u^\pm = u_1^\pm + u_2^\pm$ . Now we add one more assumption, namely that

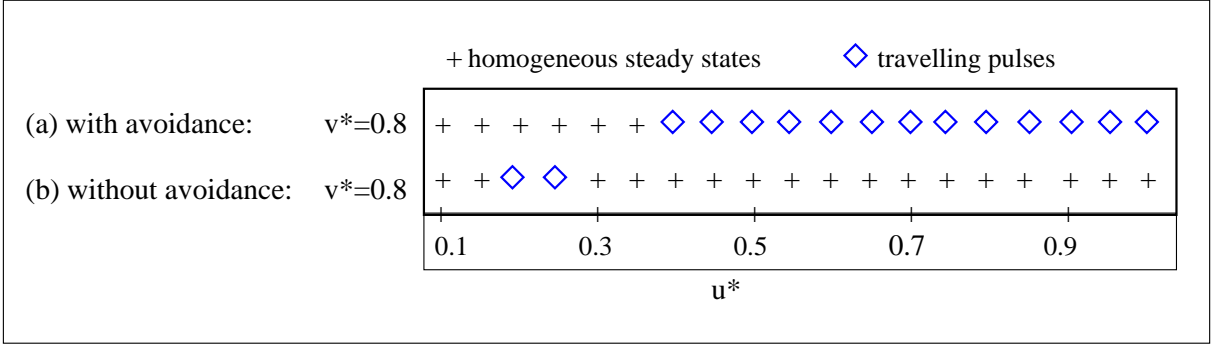


FIGURE 6. Comparison between patterns obtained (a) with avoidance behaviour (model (2.1)), and (b) without avoidance behaviour (as in [15]), for  $v^* = 0.8$  and different initial population sizes  $u^* \in (0.1, 1.0)$ .

individuals can learn, upon interactions with members of the other subpopulation ( $u_1$  or  $u_2$ ), to avoid their neighbours or not. This learning behaviour leads to transitions (at rates  $a_{12}$  and  $a_{21}$ ) between subpopulations  $u_1^\pm$  and  $u_2^\pm$ , which we assume to be proportional to the size of the subpopulations. For subpopulation  $v$  we keep the same assumptions as before. Therefore, the new model reads:

$$\frac{\partial u_1^+}{\partial t} + \gamma \frac{\partial u_1^+}{\partial x} = -\lambda_{u_1}^+[u_1^+, u_1^-, u_2^+, u_2^-]u_1^+ + \lambda_{u_1}^-[u_1^+, u_1^-, u_2^+, u_2^-]u_1^- - a_{21}u_1^+u_2 + a_{12}\frac{u_1}{2}u_2, \quad (4.1a)$$

$$\frac{\partial u_1^-}{\partial t} - \gamma \frac{\partial u_1^-}{\partial x} = \lambda_{u_1}^+[u_1^+, u_1^-, u_2^+, u_2^-]u_1^+ - \lambda_{u_1}^-[u_1^+, u_1^-, u_2^+, u_2^-]u_1^- - a_{21}u_1^-u_2 + a_{12}\frac{u_1}{2}u_2, \quad (4.1b)$$

$$\frac{\partial u_2^+}{\partial t} + \gamma \frac{\partial u_2^+}{\partial x} = -\lambda_{u_2}^+[u_1^+, u_1^-, u_2^+, u_2^-]u_2^+ + \lambda_{u_2}^-[u_1^+, u_1^-, u_2^+, u_2^-]u_2^- + a_{21}u_1\frac{u_2}{2} - a_{12}u_2^+u_1, \quad (4.1c)$$

$$\frac{\partial u_2^-}{\partial t} - \gamma \frac{\partial u_2^-}{\partial x} = \lambda_{u_2}^+[u_1^+, u_1^-, u_2^+, u_2^-]u_2^+ - \lambda_{u_2}^-[u_1^+, u_1^-, u_2^+, u_2^-]u_2^- + a_{21}u_1\frac{u_2}{2} - a_{12}u_2^-u_1, \quad (4.1d)$$

$$\frac{\partial v^+}{\partial t} + \gamma \frac{\partial v^+}{\partial x} = -\lambda_v^+[u^+, u^-, v^+, v^-]v^+ + \lambda_v^-[u^+, u^-, v^+, v^-]v^-, \quad (4.1e)$$

$$\frac{\partial v^-}{\partial t} - \gamma \frac{\partial v^-}{\partial x} = \lambda_v^+[u^+, u^-, v^+, v^-]v^+ - \lambda_v^-[u^+, u^-, v^+, v^-]v^-. \quad (4.1f)$$

Here, we denote the total densities of the two subpopulations by  $u_1 = u_1^+ + u_1^-$  and  $u_2 = u_2^+ + u_2^-$ . As before, we assume that all populations move at the same constant speed  $\gamma$ . We also assume that the  $u_2$  individuals that become  $u_1$ , have equal probability of moving left ( $u_1^-$ ) or right ( $u_1^+$ ). Similar assumption holds for the  $u_1$  individuals that become  $u_2$ . Note that the total population density is conserved. The turning rates  $\lambda_{u_1, u_2}^\pm$  are given by

$$\lambda_{u_1, u_2}^\pm = \lambda_1 + \lambda_2 f(y_r^{u_1, u_2; \pm} - y_a^{u_1, u_2; \pm} + y_{al}^{u_1, u_2; \pm}), \quad (4.2)$$

where the nonlocal interaction terms  $y_j^{u_1, u_2; \pm}$ ,  $j = r, a, a$  are described in Table 2. The turning rates  $\lambda_v^\pm$  are the same as in (2.2), while the interaction terms  $y_j^{v; \pm}$  for the  $v$  population are the same as in Table 1. The description of model (4.1) is completed by specifying also the boundary conditions. As for model (2.1), we consider the periodic boundary conditions (2.3).

Throughout the rest of this paper, we will refer to model (2.1) as the ‘‘avoidance’’ model, and to model (4.1) as the ‘‘learning’’ model. When  $u_1^\pm = 0$ , model (4.1) reduces to the model introduced in [15]. When  $u_2^\pm = 0$ , model (4.1) reduces to the ‘‘avoidance’’ model (2.1).

TABLE 2. Nonlocal social interaction terms for sub-populations  $u_1$  and  $u_2$  (which communicate via M2). We assume that  $u_1^\pm$  avoid  $v^\pm$ , while  $u_2^\pm$  tolerate  $v^\pm$ .  $K_r$ ,  $K_a$  and  $K_{al}$  are kernels describing the spatial ranges for the repulsive, attractive and alignment interactions, respectively. Throughout this study we use  $K_j(s) = (1/2\pi m_j^2) \exp(-(s - s_j)^2/(2m_j^2))$ , with  $j = r, al, a$ , and  $m_j = s_j/8$ . Finally,  $q_j$ ,  $j = r, a, al$ , are the magnitudes of the social interactions.

| Population | Interaction terms: repulsion ( $y_r^\pm$ ), attraction ( $y_a^\pm$ ), alignment ( $y_{al}^\pm$ )   |
|------------|--|
| $u_1$      | $y_r^{u_1; \pm} = \pm q_r \int_0^L K_r(s) (u_1(x+s) + u_2(x+s) - u_1(x-s) - u_2(x-s) + v(x+s) - v(x-s)) ds$ $y_a^{u_1; \pm} = \pm q_a \int_0^L K_a(s) (u_1(x+s) + u_2(x+s) - u_1(x-s) - u_2(x-s)) ds;$ $y_{al}^{u_1; \pm} = \pm q_{al} \int_0^L K_{al}(s) (u_1^-(x+s) + u_1^-(x-s) - u_1^+(x+s) - u_1^+(x-s) + u_2^-(x+s) + u_2^-(x-s) - u_2^+(x+s) - u_2^+(x-s)) ds;$   |
| $u_2$      | $y_r^{u_2; \pm} = \pm q_r \int_0^L K_r(s) (u_1(x+s) + u_2(x+s) - u_1(x-s) - u_2(x-s) + v(x+s) - v(x-s)) ds$ $y_a^{u_2; \pm} = \pm q_a \int_0^L K_a(s) (u_1(x+s) + u_2(x+s) - u_1(x-s) - u_2(x-s) + v(x+s) - v(x-s)) ds;$ $y_{al}^{u_2; \pm} = \pm q_{al} \int_0^L K_{al}(s) (u_1^-(x+s) + u_1^-(x-s) - u_1^+(x+s) - u_1^+(x-s) + u_2^-(x+s) + u_2^-(x-s) - u_2^+(x+s) - u_2^+(x-s) + v^-(x+s) + v^-(x-s) - v^+(x+s) - v^+(x-s)) ds.$ |

#### 4.1. Results for the ‘‘learning’’ model

To calculate the spatially homogeneous steady states, we first add equations (4.1a)-(4.1d). This leads to

$$-a_{21}u_1u_2 + a_{12}u_1u_2 = 0, \quad (4.3)$$

which implies that spatially homogeneous steady states exist only when  $a_{12} = a_{21}$ . This means that the rate at which population  $u_1$  learns to become tolerant (and thus to become  $u_2$ ), is that same as the rate at which population  $u_2$  learns to avoid its neighbours (and thus to become  $u_1$ ).

Let us now define the total densities for the two subpopulations that communicate via M2:  $A_1 = (1/L) \int_0^L (u_1^+(s) + u_1^-(s)) ds$  and  $A_2 = (1/L) \int_0^L (u_2^+(s) + u_2^-(s)) ds$ . Therefore,  $A = A_1 + A_2$  (with  $A$  the total density for population  $u$  described by model (2.1)). The steady-state equations for model (4.1) are

$$(u_1^+, u_1^-, u_2^+, u_2^-, v^+, v^-) = (u_1^*, A_1 - u_1^*, u_2^*, A_2 - u_2^*, v^*, B - v^*),$$

with  $u_1^*$ ,  $u_2^*$  and  $v^*$  the intersection points of the curves

$$0 = -u_1^* \left( \lambda_1 + \lambda_2 f(2q_{al}(A - 2u_1^* - 2u_2^*)) \right) + (A_1 - u_1^*) \left( \lambda_1 + \lambda_2 f(-2q_{al}(A - 2u_1^* - 2u_2^*)) \right) - a_{12}(A - A_1) \left( u_1^* - \frac{A_1}{2} \right), \quad (4.4a)$$

$$0 = -u_2^* \left( \lambda_1 + \lambda_2 f(2q_{al}(A + B - 2u_1^* - 2u_2^* - 2v^*)) \right) + (A - A_1 - u_2^*) \left( \lambda_1 + \lambda_2 f(-2q_{al}(A + B - 2u_1^* - 2u_2^* - 2v^*)) \right) - a_{12}A_1 \left( u_2^* - \frac{A_2}{2} \right), \quad (4.4b)$$

$$0 = -v^* \left( \lambda_1 + \lambda_2 f(q(A + B - 2u_1^* - 2u_2^* - 2v^*)) \right) + (B - v^*) \left( \lambda_1 + \lambda_2 f(-q(A + B - 2u_1^* - 2u_2^* - 2v^*)) \right), \quad (4.4c)$$

where  $q = q_r - q_a + q_{al}$  and  $A = A_1 + A_2$ .

Figure 7 shows the number of spatially homogeneous steady states displayed by model (4.1) for different total densities of the  $u_1$  population. Here, we keep  $A = 1.0$  and  $v^* = B/2$  fixed. We see that, in this case, irrespective of the proportion of individuals that display avoidance behaviour, system (4.4) exhibits only one steady state:  $(u_1^*, u_2^*, v^*) = (A_1/2, A/2, B/2)$ . Moreover, the value of  $a_{12} = a_{21}$  does not seem to affect the number of steady states (at least for  $a_{12} = a_{21} \in (0.1, 2)$ ). In the next section, we will investigate whether the values of  $a_{12}$  and  $a_{21}$  influence the types of the steady states.

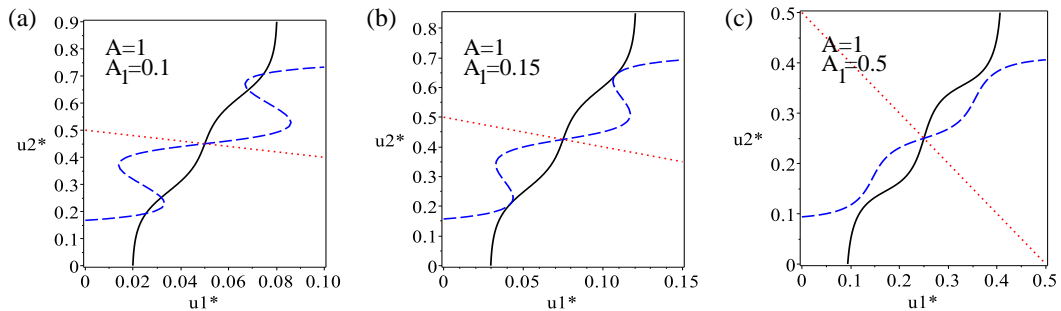


FIGURE 7. Number of spatially homogeneous steady states (s.s.) exhibited by system (4.1). The black continuous curves are solutions of equation (4.4a), the blue dashed curves are solutions of equation (4.4b), and the dotted red curves are solutions of equation (4.4c). (a)  $A_1 = 0.1$ ; (b)  $A_1 = 0.15$ ; (c)  $A_1 = 0.5$ . The rest of parameters are  $\lambda_1 = 0.2$ ,  $\lambda_2 = 0.9$ ,  $q_a = q_r = q_{al} = 2.0$ .

#### 4.1.1. Pattern formation with the “learning” model

In the following, we fix the size of  $v$  and  $u = u_1 + u_2$  populations (e.g.,  $v^* = 0.4$ ,  $u^* = 0.4$ ), and vary the initial population sizes for  $u_1$  and  $u_2$ . This allows us to investigate the density of tolerant individuals necessary to generate new aggregation patterns, or to revert the dynamics of the system to the non-avoidance case. For these parameter values, the model with avoidance behaviour shows type 1 semi-zigzag travelling pulses (see Figure 5(a)), while the model without avoidance behaviours shows zigzag pulses (see Figure 5(b))

Figure 8 shows one type of spatio-temporal patterns, namely travelling wavy pulses, obtained when  $u_1^* + u_2^* = 0.4$  and  $a_{21} = a_{12} = 0.2$ . This pattern, which was not observed in the absence of learning behaviours, represents a transition between semi-zigzag travelling pulses and zigzag pulses; see Figure 8(e). One can expect that other such transition patterns can be obtained for those parameter values where the models with avoidance and tolerance behaviours show different patterns (as seen in Figure 5 (a) and (b)). However, the purpose of this study is not to investigate all such parameter ranges; rather it is to show that learning behaviours can lead to the formation of transition patterns. Moreover, for the parameter values considered here, changing the “learning” rates  $a_{12} = a_{21} \in (0.1, 2.0)$  does not seem to lead to new patterns (not shown here). This is consistent with the effect of changing these rates on the number of steady states (as discussed previously).

We also changed  $a_{12}$  and  $a_{21}$  separate from each other, i.e., we fixed  $a_{21} = 0.2$  and increased  $a_{12}$  from 0.1 to 2.0. This case, which does not support spatially homogeneous steady states, corresponds to the assumption that one of the sub-populations  $u_1$  or  $u_2$  is more “persuasive” than the other sub-population, and can lead to a faster learning of its behaviour. Numerical results – not presented here – showed that for  $a_{12} > a_{21}$  (i.e., individuals are more likely to become  $u_1$  and avoid their neighbours), system (4.1) exhibited semi-zigzag travelling pulses of type 1 (see Figure 4(b)). In contrast, for  $a_{12} \leq a_{21}$  system (4.1) exhibited zigzag pulses.

Figure 9 shows a comparison of the spatial distribution of individuals inside travelling aggregations for three cases: (a)-(a’) in the absence of avoidance behaviours, (b)-(b’) in the presence of avoidance behaviours, and (c)-(c’) in the presence of learning and avoidance behaviours. Panels (a)-(c) show a time-space plot of the patterns, while panels (a’)-(c’) show the structure of the aggregations at a particular time step. We see that in the absence of avoidance behaviours, population  $u$  that communicates via M2 mechanism is positioned towards the middle/back of moving aggregation, while population  $v$  that communicates via M4 mechanism is positioned at the front of the moving aggregation (panel (a’)). However, the introduction of avoidance behaviours (panel (b’)) leads to an interchange in the spatial positions of  $u$  and  $v$  populations. Moreover, the introduction of learning behaviours (panel (c’)) changes

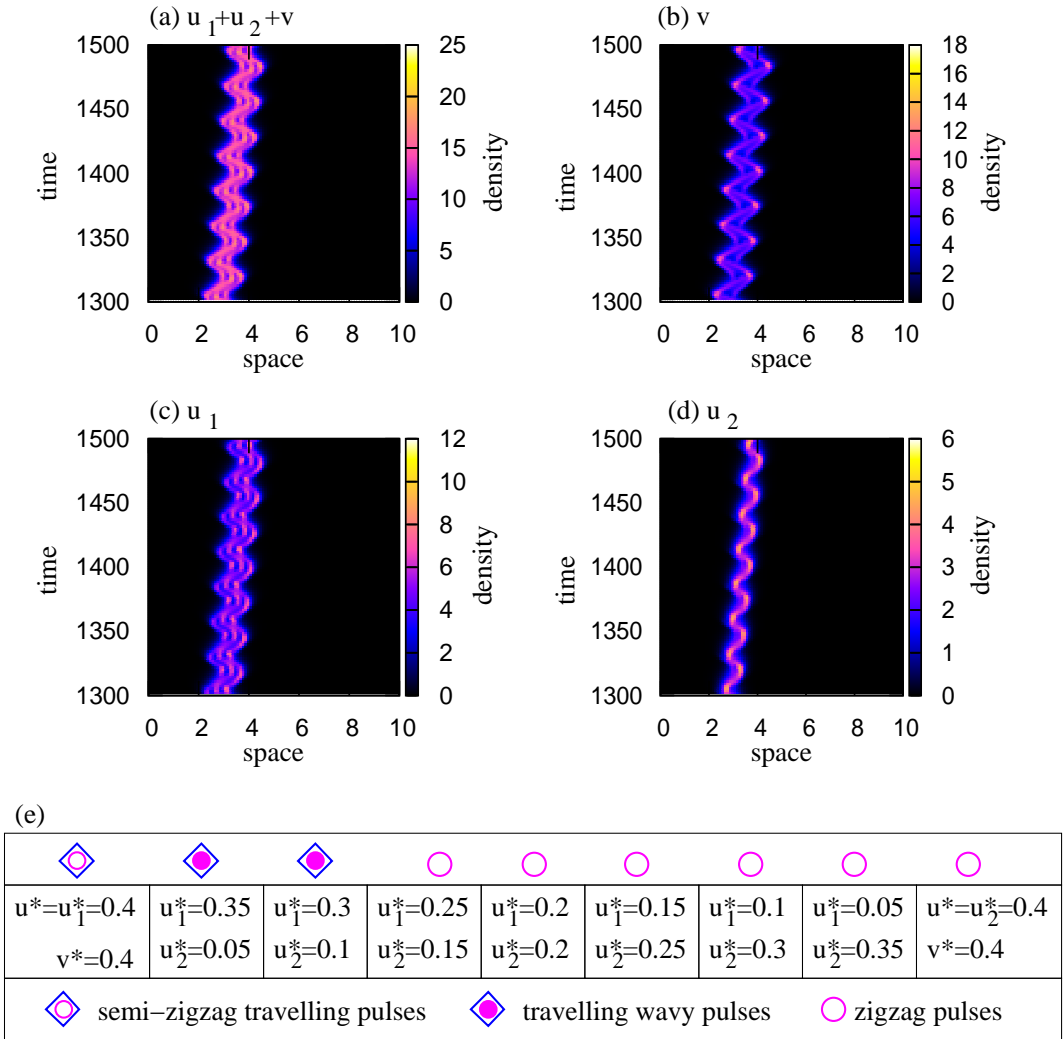


FIGURE 8. Travelling wavy pulses exhibited by model (4.1). (a) Total population density  $u_1 + u_2 + v$ ; (b) Population density  $v$ ; (c) Population density  $u_1$ ; (d) Population density  $u_2$ ; (e) Diagram with the summary of patterns obtained when  $u_1^* + u_2^* = 0.4$ ,  $v^* = 0.4$ . The parameter values are:  $a_{12} = a_{21} = 0.2$ ,  $q_a = 6.7$ ,  $q_{al} = q_r = 2$ ,  $\gamma = 0.1$ ,  $\lambda_1 = 0.2$ ,  $\lambda_2 = 0.9$ ,  $s_r = 0.25$ ,  $s_{al} = 0.5$ ,  $s_a = 0.5$ ,  $L = 10$ .

slightly the spatial distribution of the population that communicates via M2: the subpopulation  $u_1$ , which avoids  $v$ , keeps its position at the front of the moving aggregation (as in panel (b')), while the subpopulation  $u_2$ , which tolerates  $v$ , is positioned in the middle of the moving aggregation – overlapping with the  $v$  population. This is an unexpected behaviour, since it was shown in [15] that populations that communicate via M2 and M4, and which tolerate each other, segregate spatially inside moving aggregations. Since for model (4.1) these moving aggregations occur for low  $u_2$ -population sizes, in Figure 9(c') we show a 10-fold magnification of population  $u_2$ .

Note that for stationary aggregations, there is no difference between the spatial distribution of  $u$  and  $v$  populations, with or without learning behaviours (not shown here).

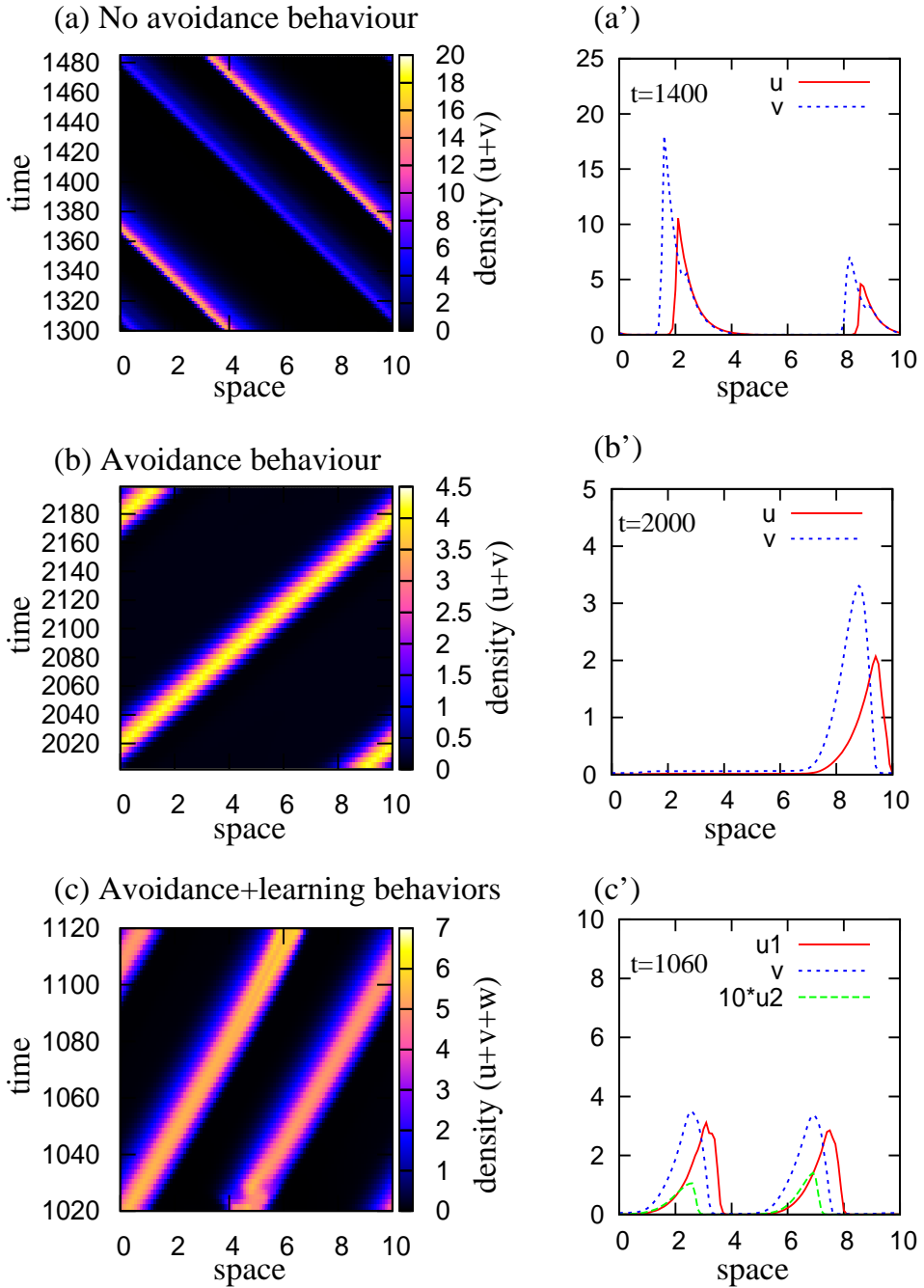


FIGURE 9. Spatial distribution of individual inside travelling aggregations in: (a)-(a') absence of any avoidance behaviours, (b)-(b') presence of avoidance behaviours, (c)-(c') presence of avoidance & learning behaviours. Initial population sizes: (a)-(a')  $u^* = 0.4$ ,  $v^* = 0.8$ ; (b)-(b')  $u^* = 0.1$ ,  $v^* = 0.2$ ; (c)-(c')  $u^* = 0.3$ ,  $v^* = 0.4$ ,  $w^* = 0.01$ . The rest of parameter values are:  $a_{12} = a_{21} = 0.2$ ,  $q_a = 6.7$ ,  $q_{al} = q_r = 2$ ,  $\gamma = 0.1$ ,  $\lambda_1 = 0.2$ ,  $\lambda_2 = 0.9$ ,  $s_r = 0.25$ ,  $s_{al} = 0.5$ ,  $s_a = 0.5$ ,  $L = 10$ .

## 5. Summary and Discussion

Mathematical models have been used intensively over the past 50 years to study the biological mechanisms that can explain the formation of biological aggregations in various species of birds, fish, bacteria, etc. So far, these models focused mainly on distance-dependent social interaction (i.e., short range repulsion from near-by neighbours, alignment with neighbours at intermediate distances and attraction to neighbours further away). Here, we proposed a mathematical model that combined distance-dependent social interactions, with the heterogeneity of communication mechanisms in biological groups and with the possible avoidance and learning behaviours caused by these communication mechanisms. This model was then employed to investigate the types of aggregation patterns exhibited by these groups.

We showed numerically that the introduction of avoidance behaviours can lead to more complex patterns compared to the case where individuals tolerate all their neighbours (case discussed in [15]). Also, the introduction of avoidance behaviours shifted the parameter ranges where certain types of patterns (e.g., travelling pulses or stationary pulses) can be obtained. Moreover, we showed that the introduction of avoidance behaviours could change the spatial distribution of individuals inside the aggregations. In particular, when individuals tolerate all their neighbours the moving aggregations were formed of M4-individuals at the front and M2-individuals at the back. This was likely the result of the communication mechanisms used for social interactions (as discussed in [15]). However, the introduction of avoidance behaviours (with M2-individuals avoiding M4-individuals) caused the M2-individuals to move towards the front of the group. In addition, the assumption that intolerant M2-individuals can learn from their more tolerant M2-neighbours lead to the spatial segregation of the M2-population: individuals that avoided  $v$  population were found at the front of the moving group, while individuals that tolerated their  $v$  neighbours were found in the middle of the moving groups (mingling with the  $v$  population). The mingling between the tolerant  $u$  and  $v$  subpopulations is unexpected, since previous studies have shown that they usually separate inside moving groups [15]. We note that the spatial segregations of populations inside stationary groups is the same for tolerant or avoiding behaviours.

While models (2.1) and (4.1) displayed a large variety of spatial and spatiotemporal patterns, we emphasise that it was not the purpose of this paper to investigate the mathematical mechanisms leading to the formation of these patterns and the transition between them. Despite the fact that such studies have started to be performed in [7, 8, 14, 17], we are still far from understanding pattern formation in these types of nonlocal hyperbolic models.

So far, the models presented in this article are only one-dimensional (modelling interactions inside domains that are longer than wide). A 2D generalisation of model (2.1) has been introduced in [19], but only for the case where individuals perceive all their neighbours (as in model M2). Due to the complexity of these two-dimensional models (of Boltzmann type), incorporating directional communication mechanisms in 2D is still an open problem. The main reason for the lack of such 2D models (either continuum or discrete) resides in the fact that it is not clear how to describe the perception (emission) of signals only from (to) those individuals that move in a particular direction in the 2D plane. However, this directionality seems to be important in nature – see, for example, the movement of Myxobacteria cells, where the frequency of cell reversal increases monotonically with the density of cells moving in the opposite direction [24].

Overall, this theoretical study emphasises the complex dynamics of biological aggregations, and the difficulty to make predictions on the types of patterns that can be displayed by these aggregations.

*Acknowledgements.* R.E. acknowledges support from an Engineering and Physical Sciences Research Council (EPSRC) First Grant number EP/K033689/1.

## References

- [1] M. Aldana, V. Dossetti, C. Huepe, V. M. Kenke, H. Larralde. *Phase transitions in systems of self-propelled agents and related network models*. Phys. Rev. Lett., 98 (2007), no. 9, 095702.

- [2] I. Barber. *Parasites and size-assortative schooling in three-spined sticklebacks*. OIKOS, 101 (2003), 331–337.
- [3] Ch. Becco, N. Vanderwalle, J. Delcourt, P. Poncin. *Experimental evidence of a structural and dynamical transition in fish school*. Physica A, 367 (2006), 487–493.
- [4] U. Börner, A. Deutsch, H. Reichenbach, M. Bär. *Rippling patterns in aggregates of myxobacteria arise from cell-cell collisions*. Phys. Rev. Lett., 89 (2002), 078101.
- [5] D.J.T. Sumpter, J. Buhl, D. Biro, I.D. Couzin. *Information transfer in moving animal groups*. Theory Biosci., 127 (2008), 177–186.
- [6] J. Buhl, D. J. T. Sumpter, I. D. Couzin, J. J. Hale, E. Despland, E. R. Miller, S. J. Simpson. *From disorder to order in marching locusts*. Science, 312 (2006), 1402–1406.
- [7] P-L. Buono, R. Eftimie. *Analysis of Hopf/Hopf bifurcations in nonlocal hyperbolic models for self-organised aggregations*. Math. Models Methods Appl. Sci., 24 (2014), 327–357.
- [8] P-L. Buono, R. Eftimie. *Codimension-two bifurcations in animal aggregation models with symmetry*. SIAM J. Appl. Dyn. Syst., 13 (2014), no. 4, 1542–1582.
- [9] José A. Carrillo, Massimo Fornasier, Giuseppe Toscani, Francesco Vecil. *Particle, kinetic, and hydrodynamic models of swarming*. Mathematical Modeling of Collective Behavior in Socio-Economic and Life Sciences (Giovanni Naldi, Lorenzo Pareschi, Giuseppe Toscani, eds.) Modeling and Simulation in Science, Engineering and Technology Birkhäuser Boston 2010, 297–336 (English).
- [10] Z. Chen, H. Liao, T. Chu. *Aggregation and splitting in self-driven swarms*. Physica A, 391 (2012), 3988–3994.
- [11] Y.-L. Chuang, M.R. D’Orsogna, D. Marthaler, A.L. Bertozzi, L.S. Chayes. *State transitions and the continuum limit for a 2d interacting, self-propelled particle system*. Physica D, 232 (2007), 33–47.
- [12] A. Czirik, M. Vicsek, T. Vicsek. *Collective motion of organisms in three dimensions*. Physica A, 264 (1999), 299–304.
- [13] R. Eftimie. *Hyperbolic and kinetic models for self-organized biological aggregations and movement: a brief review*. J. Math. Biol., 65 (2012), no. 1, 35–75.
- [14] R. Eftimie. *The effect of different communication mechanisms on the movement and structure of self-organised aggregations*. Math. Model. Nat. Phenom., 7 (2013), no. 2, 32–51.
- [15] R. Eftimie. *Simultaneous use of different communication mechanisms leads to spatial sorting and unexpected collective behaviours in animal groups*. J. Theor. Biol., 337 (2013), 42–53.
- [16] R. Eftimie, G. de Vries, M.A. Lewis. *Complex spatial group patterns result from different animal communication mechanisms*. Proc. Natl. Acad. Sci., 104 (2007), no. 17, 6974–6979.
- [17] R. Eftimie, G. de Vries, M.A. Lewis. *Weakly nonlinear analysis of a hyperbolic model for animal group formation*. J. Math. Biol., 59 (2009), 37–74.
- [18] R. Eftimie, G. de Vries, M.A. Lewis, F. Lutscher. *Modeling group formation and activity patterns in self-organizing collectives of individuals*. Bull. Math. Biol., 69 (2007), no. 5, 1537–1566.
- [19] R.C. Fetecau. *Collective behavior of biological aggregations in two dimensions: a nonlocal kinetic model*. Math. Models Methods Appl. Sci., 21 (2011), no. 7, 1539.
- [20] F. Ginelli, H. Chaté. *Relevance of metric-free interactions in flocking phenomena*. Phys. Rev. Lett., 105 (2010), 168103.
- [21] E. Goodale, G. Beauchamp, R.D. Magrath, J.C. Nieh, G.D. Ruxton. *Interspecific information transfer influences animal community structure*. Trends Ecol. Evol., 25 (2010), no. 6, 354–361.
- [22] N.M. Harrison, M.J. Whitehouse. *Mixed-species flocks: an example of niche construction?*. Anim. Behav., 81 (2011), no. 4, 675–682.
- [23] J.K. Hellerstein, D. Newmark. *Workplace segregation in the United States: race, ethnicity, and skill*. The review of Economics and Statistics, 90 (2008), no. 3, 459–477.
- [24] O. Igoshin, A. Mogilner, R. Welch, D. Kaiser, G. Oster. *Pattern formation and traveling waves in myxobacteria: Theory and modeling*. Proc. Natl. Acad. Sci. USA, 98 (2001), 14913–14918.
- [25] J. Krause. *The relationship between foraging and shoal position in a mixed shoal of roach (*Rutilus rutilus*) and chub (*Leuciscus cephalus*): a field study*. Oecologia, 93 (1993), 356–359.
- [26] J.R. Krebs. *Social learning and the significance of mixed-species flocks of chickadees (*Parus spp.*)*. Can. J. Zool., 51 (1973), no. 12, 1275–1288.
- [27] P.J.O. Miller. *Mixed-directionality of killer whale stereotyped calls: a direction of movement cue?*. Behav. Ecol. Socio-biol., 52 (2002), 262–270.
- [28] R. Muzinic. *On the shoaling behaviour of sardines (*Sardina pilchardus*) in aquaria*. J. Cons. Int. Expl. Mer., 37 (1977), 147–155.
- [29] M. Nagy, Z. Akos, D. Biro, T. Vicsek. *Hierarchical group dynamics in pigeon flocks*. Nature, 464 (2010), 890–893.
- [30] J.K. Parrish. *Layering with depth in a hetero-specific fish aggregation*. Env. Biol. Fishes, 26 (1989), 79–86.
- [31] P.H.C. Pereira, J.L.L. Feitosa, D.V. Medeiros, B.P. Ferreira. *Reef fishes foraging facilitation behaviour: increasing the access to a food resource*. Acta Ethologica, 16 (2013), no. 1, 53–56.
- [32] C.W. Reynolds. *Flocks, herds and schools: A distributed behavioral model*. Computer Graphics, 21 (1987), 25–34.
- [33] R.M. Seyfarth, D.L. Cheney, P. Marler. *Monkey responses to three different alarm calls: evidence of predator classification and semantic communication*. Science, 210 (1980), no. 4471, 801–803.
- [34] H. Sridhar, G. Beauchamp, K. Shanker. *Why do birds participate in mixed-species foraging flocks? A large-scale synthesis*. Anim. Behav., 78 (2009), no. 2, 337–347.
- [35] D.J.T. Sumpter. *The principles of collective animal behaviour*. Phil. Trans. R. Soc. B, 361 (2006), 5–22.
- [36] T. Vicsek, A. Czirik, E. Ben-Jacob, I. Cohen, O. Shochet. *Novel type of phase transition in a system of self-driven particles*. Phys. Rev. Lett., 75 (1995), no. 6, 1226–1229.

- [37] T. Vicsek, A. Czirok, I.J. Farkas, D. Helbing. *Application of statistical mechanics to collective motion in biology*. Physica A, 274 (1999), 182–189.
- [38] G. Vines. *Spatial consequences of aggressive behaviour in flocks of oystercatchers, Haematopus Ostralegus L.* Anim. Behav., 28 (1980), no. 4, 1175–1183.
- [39] D.P. Whitfield. *Plumage variability, status signalling and individual recognition in avian flocks*. Trends in Ecology & Evolution, 2 (1987), 13–18.
- [40] S.R. Witkin. *The importance of directional sound radiation in avian vocalization*. The Condor, 79 (1977), 490–493.
- [41] A.J. Wood, G.J. Ackland. *Evolving the selfish herd: emergence of distinct aggregating strategies in an individual-based model*. Proc. R. Soc. B, 274 (2007), 1637–1642.